ResearchGate

See discussions, stats, and author profiles for this publication at: https://www.researchgate.net/publication/13339950

Theory of Auger core-valence-valence processes in simple metals. I. Total yields and core-level lifetime widths

Article *in* Physical review. B, Condensed matter · March 1989

DOI: 10.1103/PhysRevB.39.3489 · Source: PubMed

CITATIONS
56

READS
14

3 authors, including:

Carl-Olof Almbladh
Lund University
72 PUBLICATIONS **2,561** CITATIONS
SEE PROFILE

Alvaro Luis Morales
University of Antioquia
119 PUBLICATIONS **1,079** CITATIONS
SEE PROFILE

Some of the authors of this publication are also working on these related projects:

variational many-body theory View project

Nonlinear optical properties in low dimensional systems. View project

All content following this page was uploaded by Carl-Olof Almbladh on 18 February 2016.

The user has requested enhancement of the downloaded file. All in-text references underlined in blue are added to the original document and are linked to publications on ResearchGate, letting you access and read them immediately.

Theory of Auger core-valence-valence processes in simple metals. I. Total yields and core-level lifetime widths

C.-O. Almbladh and A. L. Morales*
Department of Theoretical Physics, Lund University, Sölvegatan 14A, S-223 62 Lund, Sweden

G. Grossmann
Department of Solid State Physics, Lund University, Sölvegatan 14, S-223 62 Lund, Sweden
(Received 11 April 1988)

There is a considerable disagreement in the literature on the description of lifetime effects arising from core-valence transitions in solids. We calculate here Auger and radiative widths of shallow core levels in Li, Be, Na, Mg, and Al with use of principles consistent with dynamical theories of secondary-emission processes developed earlier. The lifetime has no simple relation to the usual self-energy but is instead directly related to emission yields. The problem of choosing reliable approximations for Auger rates and matrix elements is analyzed theoretically and computationally. We also comment on some earlier approaches. Much of our discussion pertains also to calculations of Auger line shapes from first principles. For long hole lifetimes the total and partial level widths obey an initial-state rule and follow from wave functions perturbed by a static core hole. To obtain these impurity wave functions we perform self-consistent supercell calculations. The core-hole screening increases the Auger rates by factors of the order 2–4 compared with results from ground-state orbitals but has never been properly included before. The width of the 1*s* level in Li is rather accurately known because it monitors large effects of incomplete lattice relaxation. For Li we obtain here a width 17 meV in excellent agreement with the value 16 meV deduced earlier from measurements by Callcott *et al.*

I. INTRODUCTION

In this and the following paper we shall address a number of what we believe to be unresolved questions in the description of core-valence-valence (*CVV*) transitions in metals. In the present paper we consider the principles of how core-level lifetime widths of shallow core levels in metals should be obtained theoretically and present *ab initio* results based on the linear muffin-tin-orbital (LMTO) repeated-cluster method. In the following paper[1] we will be concerned with the question to what extent Auger line shapes may be obtained from strict one-electron theory, possibly corrected by surface and mean-free-path effects, and the role of dynamical effects connected with the sudden disappearance of the core hole in the final state of the process. Throughout these two papers we will confine ourselves to the simple metals Li, Be, Na, Mg, and Al. Preliminary results have been reported earlier at international conferences.[2]

The lifetime widths of, say, the 1*s* core level in Li might seem to be a rather uninteresting quantity, giving rise to a mere broadening of a deep-level spectrum. While this is the case for x-ray-photoemission (XPS) and soft-x-ray-absorption (SXA) spectroscopy connected with the core-hole–*creation* process, the lifetime enters in a more interesting way in the description of secondary spectra such as x-ray-emission and Auger emission spectra connected with the subsequent decay of the core hole. When the core-hole lifetime is not too long or not too short compared to the time needed for the system to relax in the core-hole potential, interesting dynamical effects originating from partial core-hole relaxation have been predicted and observed in both x-ray-emission and Auger emission spectra.[3–10] The core-hole lifetime monitors the degree of relaxation seen in these secondary emission spectra. In this regard the lifetime of holes in the uppermost core shell in a simple metal is of special interest since these lifetimes are generally believed to be of the same order as the lattice relaxation time, i.e., corresponding to widths of the order 10^{-2} eV. The core-hole lifetime also plays an important role in resonant photoemission processes in which direct and indirect channels involving core-hole states interfere. In the current description of these phenomena the lifetime has a precise definition, and an accurate calculation provides a test of the internal consistency. In this way one can also obtain measures on the accuracy by which transition matrix elements of importance to line shapes can be obtained.

Previous calculations[11–14] of core-level lifetime widths in simple metal have all been based on crude approximations of wave functions and matrix elements and have given conflicting results. Our work is intended to show the importance of using accurate wave functions and proper descriptions of the ejected Auger electron. Of more importance is that some previous works are from a conceptual point of view in clear conflict with, by now,

 ©1989 The American Physical Society

well-established theories of lifetime effects in solids.[3–9,15–17] Conceptual difficulties arise mainly for core levels that decay via core-valence transitions, since in that case the valence electrons play a dual role in that they participate both in the core-hole annihilation and the core-hole relaxation processes. According to these general theories, which are developed to cope with dynamical effects in secondary spectra and with resonance phenomena, the lifetime width is to be identified with the core-hole annihilation rate, not with the core-electron self-energy as has been done in most previous calculations. Due to, e.g., shakeup of electron-hole pairs, the latter quantity would be nonzero even if the core hole did not decay at all. The identification of the lifetime widths with a total annihilation rate (or total yield), on the other hand, is exactly what simple physical intuition would suggest. Further, one can show that for lifetimes which are long compared to the relaxation time, the widths (Γ) should be evaluated from a wave function $|0^*\rangle$ with a completely relaxed core hole. Introducing a "decay" operator $\hat{\Gamma}$ which gives the core-hole annihilation rate for arbitrary (core-hole) N-electron states, we thus have

$$\Gamma \equiv \Gamma_* = \langle 0^* | \hat{\Gamma} | 0^* \rangle \ . \tag{1}$$

Specializing to a one-electron picture and to Auger decay, Eq. (1) gives

$$\Gamma_A = \int D_A(\varepsilon) d\varepsilon \ , \tag{2}$$

where

$$D_A(\varepsilon) = 2\pi \sum_{k,l}^{\text{occ}} \sum_{k_A} (|\langle kl|v|cA\rangle|^2 - \langle kl|v|Ac\rangle^* \langle kl|v|cA\rangle) \delta(\varepsilon_k + \varepsilon_l - \varepsilon_c - \varepsilon_{k_A}) \delta(\varepsilon - \varepsilon_{k_A}) \tag{3}$$

is the usual one-electron expression for the Auger rate with one important exception—all orbitals are perturbed by the core hole and no longer have Bloch symmetry. [In Eq. (3) v is the Coulomb interaction, k and l denote valence states, A is the ejected Auger electron, and c the core electron. We use units such that $e^2 = \hbar = m = 1$.]

In this work we will evaluate the widths according to the prescription above, Eqs. (1)–(3). Our procedure is related to that used recently by Green and Jennison[18] to obtain total yields in alkali halides. We use orbitals obtained from self-consistent calculations on a repeated cluster where every 16th atom is a core-hole atom, a method used earlier by von Barth and Grossman.[19] For completeness we also calculate the radiative width Γ_r in order to obtain the fluorescence yield (Γ_r/Γ). Traditionally one has in most calculations of core-level widths in metals used a screened and in many cases a statically screened interaction for evaluating the Auger matrix elements. On the other hand, one has in more realistic calculations of Auger spectra been using an *unscreened* interaction.[18–21] Here we will give what we think are convincing arguments that the latter choice is, in fact, the appropriate one for the systems considered here (Sec. II).

The remaining part of this paper is organized as follows. In Sec. II we briefly describe the main physical ideas behind our treatment of decay process, motivate our approximations from a many-body theoretical point of view, and discuss some of the previous works. Apart from this section, which may be omitted for readers interested only in our results, this paper deals mainly with one-electron concepts. In Secs. III–V we outline the principles of how our effective one-electron expressions for Auger and radiative rates are evaluated in practice. Our results are described in Sec. VI, and in Sec. VII we give some concluding remarks.

II. THEORY OF CORE-HOLE LIFETIME EFFECTS IN SOLIDS

A. General background

The theoretical description of lifetime effects in solids has been reviewed an extended in great detail recently by Almbladh and Hedin,[9] which relieves us from going into too much detail here. However, in order to motivate our approximations and to discuss some previous works it will be necessary to describe the main physical ideas.

A conceptually clear way to treat lifetime effects in solids is to split the "exact" Hamiltonian H into a part H_0 without lifetime effects and a perturbation V.[3–9] The unperturbed part contains all electron-electron interactions, except those terms which make the core hole unstable, and is treated in a formally exact way. (Approximations for this part are chosen at a later stage.) The perturbation contains the remaining terms and consists of an Auger part V_A and a coupling V_r to the radiation field. In the present case we confine ourselves to processes involving one core level at a specific site, which allows us to write

$$H_0 = H_v + \varepsilon_c^0 n_c + V_v(1 - n_c) + H_{\text{phot}} \tag{4}$$

in the subspaces corresponding to a filled ($n_c = 1$) and an unfilled ($n_c = 0$) core level, respectively. In Eq. (4), H_v describes in principle the fully interacting valence system when all core levels are filled, ε_c^0 is an unrenormalized core-electron energy without solid-state effects and can be identified with that of a free ion in vacuum (see, e.g., Ref. 9, p. 646), V_v is the nonlifetime core-valence coupling which gives rise to particle-hole and plasmon shakeup, core-level relaxation shifts, etc. H_{phot} is the free radiation field which needs to be included only when radiative

core-hole decay is considered. The lifetime parts V_A and V_r contain only terms nondiagonal in core-level occupancies and can be written

$$V_A=\sum_{k,l,A}\langle kl|v|cA\rangle c_k^\dagger c_l^\dagger c_A b+\text{H.c.}\ , \tag{5}$$

$$V_r=\sum_{k,q}(2\pi\alpha/|\mathbf{q}|)^{1/2}\langle k|-i\boldsymbol{\varepsilon}_q\cdot\nabla|c\rangle c^\dagger b a_q+\text{H.c.}$$
$$\equiv\sum_q T_r(q)a_q+\text{H.c.} \tag{6}$$

Here α is the fine-structure constant, c_k and b are, respectively, valence- and core-electron operators, a_q is a photon operator, and q is short for the photon wave vector and polarization.

The model lifetime problem expressed in Eqs. (4)–(6) can be solved in closed form both for primary (XPS, SXA) and secondary emission spectra by at least three seemingly rather different techniques:[22] infinite-order perturbation theory[23] extended to the case of a continuous manifold of decaying states,[4,5,9] scattering theory assisted by a Feshbach[24] projection technique,[6–9] and by Fano theory.[15,16] As was indicated in the Introduction, the solution can conveniently be expressed in terms of a decay operator[8,9]

$$\hat{\Gamma}(E)=2\pi V\delta(E-H_0)V\ . \tag{7}$$

Neglecting unimportant cross terms we can decompose the decay operator into an Auger ($\hat{\Gamma}_A$) and a radiative ($\hat{\Gamma}_r$) part obtained by replacing the full V in Eq. (7) by its Auger and radiative part, respectively.

When the decay operator acts on a state Ψ with a core hole its radiative or Auger part fills the core level and couples to no-hole final states. Thus we see that $\langle\Psi|\hat{\Gamma}|\Psi\rangle$ gives a core-hole annihilation rate according to

$$\dot{w}(\Psi)=2\pi\sum_f|\langle f,\ n_c=1|V|\Psi\rangle|^2\delta(E-E_f(n_c=1))\ .$$

When the core hole decays via intracore processes, $\hat{\Gamma}$ can be taken as a c-number as far as the valence electrons are concerned, $\hat{\Gamma}=\Gamma$, and the proper definition of the lifetime width is obvious. When $\hat{\Gamma}$ involves only core-valence processes, the valence electrons take part in both the core-hole screening as well as the core-hole annihilation processes, and as a consequence the true lifetime effects are more difficult to sort out. To obtain a sensible definition of the hole lifetime in this latter case it is useful to study the time development of a state $b|0\rangle$ corresponding to a sudden removal of a core electron out of the ground state at $t=0$. At a later time t the projection of this state on the hole subspace is

$$\Psi(t)\equiv P(n_c=0)e^{-iHt}b|0\rangle=b^\dagger be^{-iHt}b|0\rangle\ .$$

The norm

$$p(t)=\langle 0|b^\dagger(0)b(t)b^\dagger(t)b(0)|0\rangle$$

of this state, which has been termed "decay function," gives the probability that the core hole has not yet been filled at a later time t. At $t=0$, $p(t)=1$ and $p(\infty)=0$. Clearly the integral of $p(t)$ between zero time and infinity gives a measure of the core-hole annihilation rate, which leads us to the identification $\Gamma^{-1}=\int_0^\infty p(t)dt$. This width is the usual full width at half maximum (FWHM) width in the case of exponential decay. One can further show that except for very short times of the order ε_c^{-1} the time derivative of $p(t)$ is $\dot{p}(t)=-\langle\Psi(t)|\hat{\Gamma}|\Psi(t)\rangle$, which allows us to rewrite the lifetime width as

$$\Gamma=\frac{\int_0^\infty\langle\Psi(t)|\hat{\Gamma}|\Psi(t)\rangle dt}{\int_0^\infty p(t)dt}\ . \tag{8}$$

The partial level widths Γ_A and Γ_r may be defined in an analogous manner as

$$\Gamma_\nu=\frac{\int_0^\infty\langle\Psi(t)|\hat{\Gamma}_\nu|\Psi(t)\rangle dt}{\int_0^\infty p(t)dt}\ ,\quad \nu=A,r \tag{9}$$

and can be shown to give the correct Auger and radiative yields Γ_A/Γ and Γ_r/Γ, respectively.

Here we will mainly be concerned with the case when the core-hole lifetime Γ^{-1} is long compared with the valence-electron relaxation time τ (which is of the order of a reciprocal Fermi or plasmon energy). In this case one can show from quite general arguments as well as from model studies that expectation values of operators which like $\hat{\Gamma}$ only probe the system near the core hole factorize as[4,5,8,9]

$$\langle\Psi(t)|\hat{\Gamma}|\Psi(t)\rangle\sim\langle\Psi(t)|\Psi(t)\rangle\langle 0^*|\hat{\Gamma}|0^*\rangle$$

for times which are long compared to τ. Here $|0^*\rangle$ is the fully relaxed core-hole state, i.e., the lowest state of H_0 in the subspace $n_c=0$. Neglecting deviations from this behavior for shorter times, Eqs. (8) and (9) finally give

$$\Gamma=\langle 0^*|\hat{\Gamma}|0^*\rangle,\quad \Gamma_\nu=\langle 0^*|\hat{\Gamma}_\nu|0^*\rangle\ . \tag{10}$$

Thus one has for long lifetimes an *initial-state rule* for lifetime widths and total yields, a physically rather sensible result.

Experimentally, lifetime widths are deduced assuming that the core-hole lifetime enters only via an additional Lorentzian broadening. Thus, e.g., the core-electron spectrum is assumed to have the form

$$A_c(\varepsilon)=\int\frac{d\varepsilon'}{2\pi}A_c^\infty(\varepsilon-\varepsilon')D_\Gamma(\varepsilon') \tag{11}$$

in terms of a fictitious spectrum $A_c^\infty(\varepsilon)$ without lifetime effects and a broadening function $D_\Gamma(\varepsilon)=\Gamma/(\varepsilon^2+\Gamma^2/4)$. The spectra A_c and A_c^∞ are formally defined as the imaginary parts of the corresponding core-electron Green's functions and can be written

$$A_c(\varepsilon)=\frac{1}{\pi}\text{Im}\langle 0|b^\dagger(\varepsilon-E_0+H-i\eta)^{-1}b|0\rangle$$
$$=\frac{1}{\pi}\text{Im}\langle 0|b^\dagger[\varepsilon-E_0+H_0-i\hat{\Gamma}(E_0-\varepsilon)/2]^{-1}b|0\rangle\ , \tag{12}$$

$$A_c^\infty(\varepsilon)=\frac{1}{\pi}\text{Im}\langle 0|b^\dagger(\varepsilon-E_0+H_0-i\eta)^{-1}b|0\rangle \tag{13}$$

(E_0 is the N-electron ground-state energy). The second equality in Eq. (12) follows by applying Feshbach projector algebra and by neglecting a small "Lamb shift" of the core-electron energy. At this point it is worth emphasizing that due to the interaction in H_0, the infinite-lifetime spectrum is *not* a δ-function line, but is instead a continuous distribution. Thus already A_c^{∞} contains broadenings, and in fact, for shallow core levels the major part of them (phonon broadening, plasmon- and particle-hole shakeup, etc.). Considering intracore decay processes, we may take $\hat{\Gamma}$ to be a c-number, and the convolution law in Eq. (11) readily follows. Interestingly enough, the convolution law also follows for core-valence processes, provided the decay is slow compared to the valence-electron relaxation process and provided we define Γ according to Eq. (10) (see Ref. 9 for further details). Thus we see that our definition of core-hole lifetime widths is in close correspondence with current experimental practice.

B. Relation to diagrams

The formalism of the preceding subsection is useful for establishing general results such as the initial-state rule for lifetime widths, but systematic expansions of the resulting expressions in powers of the interparticle interaction are most easily obtained using diagrams or by related techniques. In the present case we wish to consider a specific subclass of final states, namely those with no real core hole. Problems involving selective summations of final states lead in a natural way to path-ordered rather than time-ordered diagrams.

The quantity we wish to study is the core-electron spectral function $A_c(\varepsilon)$. Going to time space we write $A_c(\varepsilon)$ as

$$A_c(\varepsilon)=\frac{-i}{2\pi}\int dt\, g_<(t)e^{i\varepsilon t} ,$$

where $g_<(t)=i\langle 0|b^{\dagger}(0)b(t)|0\rangle$ can be computed directly from path-ordered diagrams. In the path-ordered technique[25] the usual time ordering is replaced by ordering along a time path going from $-\infty$ to $+\infty$ and then back to $-\infty$. Since Wick's theorem does not depend on the particular ordering principle used, the usual rules for evaluating diagrams remain valid provided we observe that all points on the negative time-ordering path going from $+\infty$ to $-\infty$ (labeled $-$) are considered ahead of all times on the positive time-ordering path (labeled $+$). The function $g_<$ can be written

$$g_<(\varepsilon)=g_c(\varepsilon)\Sigma_<(\varepsilon)g_{\bar{c}}(\varepsilon) \tag{14}$$

in terms of the self-energy $\Sigma_<(t)$ $[=\Sigma(t_+,0_-)]$ and the core propagators g_c and $g_{\bar{c}}$ corresponding to positive and negative time ordering, respectively. Below the Fermi level (μ), $\Sigma_<(\varepsilon)=-2i\,\mathrm{Im}\Sigma_c(\varepsilon)$, where $\Sigma_c(\varepsilon)$ is the usual time-ordered self-energy. Using this property it is not difficult to show that Eq. (14) is equivalent to the more common expression

$$A_c(\varepsilon)=\frac{1}{\pi}\mathrm{Im}g_c(\varepsilon) .$$

In the expansion of $g_<$ and $\Sigma_<$ in interacting propagators and screened interactions, fermion and interaction lines connecting points with opposite time ordering represent real excitations in the final state (see, e.g., Ref. 26). Thus we see that in the expansion of $\Sigma_<$ we can isolate the lifetime part by keeping only those skeleton diagrams which have no real core hole in the final state, i.e., those with no (full) $g_<$ line. Extending this principle further we see that the radiative part ($\Sigma_<^r$) and the Auger part ($\Sigma_<^A$) correspond to lifetime diagrams with and without a real photon, respectively. It is now natural to take the lifetime widths as

$$\Gamma_A=i\Sigma_<^A(\varepsilon_c),\quad \Gamma_r=i\Sigma_<^r(\varepsilon_c) . \tag{15}$$

It is clear from their definition that these quantities give, respectively, the (intrinsic) Auger and radiative yields.

The definition above allows, in fact, for an independent justification of the results summarized in the preceding subsection by means of diagrams. Here, however, we will instead rely on the previous results and directly study the quantity $\langle 0^*|\hat{\Gamma}|0^*\rangle$. We limit the discussion to the Auger part, as the radiative part can be handled in an analogous manner. It is quite easy to see that the relaxed Auger width $\langle 0^*|\hat{\Gamma}_A|0^*\rangle$ is obtained from a subclass of diagrams for $\Sigma_<^A$ by replacing all ground-state propagators by the corresponding ones which are perturbed by a static core hole. The subclass in question consists of the diagrams without any core lines. The lowest-order diagrams are given in Fig. 1. In mean-field theory these are to be evaluated with independent-electron propagators for the core-hole system. Choosing a one-particle basis which makes these propagators diagonal we find that the first diagram [Fig. 1(a)] gives

$$i\Sigma_<^{1(a)}(\varepsilon_c)=-i\sum_{k,l,A}|\langle kl|v|cA\rangle|^2 \times\int dt\, G_k^<(t)G_l^<(t)G_A^>(-t)e^{i\varepsilon_c t} ,$$

which is readily found to reproduce the direct part of the independent-electron result in Eqs. (1)–(3) (G is a valence-electron propagator). In a similar way we find that the diagram to the right gives the exchange part. Let us now consider the effects of replacing the bare interaction v by the screened one [$W(\omega)$]. An easy calculation shows that the diagram to the left now gives the contribution

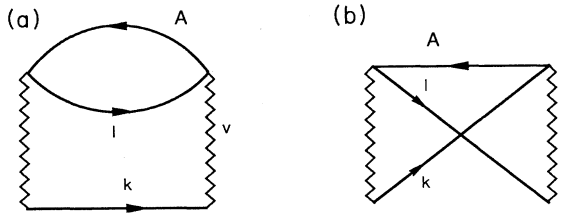

FIG. 1. The lowest-order diagrams for the Auger process.

$$2\pi \sum_{kl}^{\text{occ}} \sum_{k_A} |\langle kl|W_c(\varepsilon_k-\varepsilon_c)|cA\rangle|^2 \delta(\varepsilon_k+\varepsilon_l-\varepsilon_c-\varepsilon_A) .$$

A similar expression is obtained from the exchange graph. Since the energy transfer in W is of the order of a core-electron energy, the screening is of the order $\omega_p^2/\varepsilon_c^2$ and can safely be neglected. We next replace the independent-electron propagators by their interacting counterpart,

$$G_<(\varepsilon)=2\pi i A(\varepsilon)\Theta(\mu-\varepsilon) ,$$

$$G_>(\varepsilon)=-2\pi i A(\varepsilon)\Theta(\varepsilon-\mu) .$$

In this case we can no longer choose a one-electron basis so as to make the spectral density $A(\varepsilon)$ diagonal for all energies. The interactions, however, do not change the total weight of the diagonal part, $\int \langle k|A(\varepsilon)|k\rangle d\varepsilon$, which thus equals unity as in the case of noninteracting electrons. Further, the off-diagonal elements have zero total weight. The lifetime width involves integrals of the spectral densities of the valence electrons and the Auger electron below and above the Fermi level, respectively, and therefore we expect only minor changes from the self-consistent-field (SCF) result. The interactions do, however, give important modifications of the line shape, shifting part of the oscillator strength from the main band to plasmon satellites.[27]

Evaluating the widths of the properly renormalized versions of the diagrams in Fig. 1 corresponds to taking the density of states of two valence holes as the convolution of two one-hole densities of states. Experiments suggest that this is a very reasonable assumption for simple metals, but it is certainly not valid for narrow-band systems, as has been demonstrated both experimentally and theoretically.[28] In such systems we might expect important effects also for the total Auger rate from (valence-) hole-hole interactions.

It remains to discuss the choice of core-electron energy in the resulting mean-field expression for the yield Eqs. (1)–(3). The proper choice is of importance for very shallow core levels like the $L_{2,3}$ level in Na. It follows readily from the structure of the theory that the correct energy in the general expressions, Eq. (15), is the difference between the lowest energies of H_0 in Eq. (4) in the subspaces $n_c=0$ and $n_c=1$, respectively. This energy contains relaxation corrections to the one-electron eigenvalue. Choosing H_0 as independent-electron Hamiltonians in the two subspaces we obtain the relaxation shift as a sum of eigenvalue shifts for the valence states, which is a rather crude approximation. Mean-field theory is variational and does not correspond to well-defined Hamiltonians for $n_c=1$ and $n_c=0$. In this case the physically obvious choice is to take the core energy as a difference between the two variational estimates in the respective subspaces. This "ΔSCF" energy agrees with the experiment within typically 1 eV for the systems considered here, and consequently it will not affect our results in any important way if we instead use the experimental core energy.

We end this section with some remarks on previous work by Glick and Hagen[12] (GH) and by Bose.[13] The two works are similar to their approach so we confine the discussion to the first paper. GH attempted to obtain a lifetime width by including the diagram in Fig. 2(a). Here the double-dashed line represents a core propagator renormalized only with respect to lifetime effects, and was taken as

$$g_c^{(d)}=\frac{1}{\varepsilon-\varepsilon_c-i\Gamma/2} . \tag{16}$$

We first note that the diagram 2(a) is contained in the nonlifetime skeleton diagram to the right [diagram 2(b)], which corresponds to the well-known "GW" approximation,[29] and is thus not related to an Auger yield. When evaluated with the decaying propagator in Eq. (16), diagram 2(a) gives the result $\Sigma_\infty^{2(a)}(\varepsilon-i\Gamma/2)$ in terms of the corresponding result obtained with the zeroth-order propagator. [Note that $\Sigma_\infty^{2(a)}(\varepsilon)$ contains no hole lifetime.] To the imaginary part of this diagram GH then add the proper lifetime part (Γ_0) from the lowest-order Auger diagrams of Fig. 1, evaluated in a simple approximation, and finally take the lifetime width as

$$\Gamma=\Gamma_0+2\,\mathrm{Im}\Sigma_\infty^{2(a)}(\varepsilon_c-i\Gamma/2) . \tag{17}$$

Extending the GH principle also to higher-order diagrams would lead to the result

$$\Gamma=\Gamma_0+2\,\mathrm{Im}\Sigma_\infty(\varepsilon_c-i\Gamma/2) \tag{18}$$

where Σ_∞ is the entire self-energy of the core propagator g_∞ without lifetime effects, a clearly absurd result. In fact, Eq. (18) represents the entire core-level width[5] of which the proper lifetime part (Γ_0) is only a small fraction for shallow levels.

The GH prescription is not only in conflict with fundamental principles, but it also violates the convolution law in Eq. (11), in disagreement with experimental findings. As is well known, this law corresponds, in a diagrammatic language, to the following procedure. We first consider the nonlifetime core propagator g_∞, expanded to all orders. We then in each diagram replace the zeroth-order core propagator by its counterpart $g_c^{(d)}$ in Eq. (16), renormalized only with respect to the core-hole lifetime effects. The result then represents the full core-electron propagator and gives, as is readily shown, the convolution law in Eq. (11).[5] Applying this principle with GH's definition of

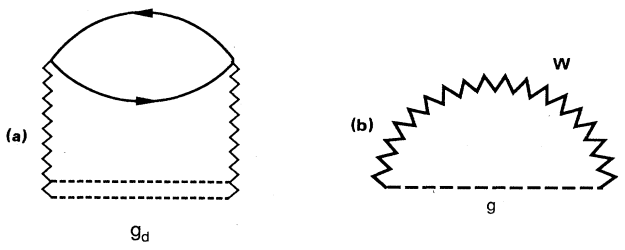

FIG. 2. (a) A lifetime diagram according to Refs. 12 and 13. The double-dashed line represents a core propagator renormalized with respect to decay processes. (b) The skeleton which contains the diagram in (a).

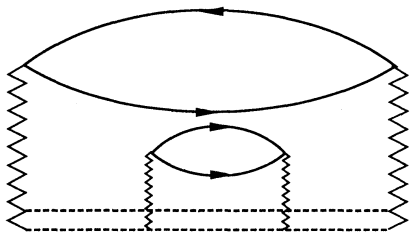

FIG. 3. A diagram which is double counted when one tries to reconcile the theory in Refs. 12 and 13 with a convolution law.

lifetime parts, however, gives a multiple double counting of diagrams of the type indicated in Fig. 3. Extending the GH principle as in Eq. (18) leads in a similar way to a multiple double counting of all diagrams contained in the nonlifetime propagator g_∞.

III. ONE-PARTICLE THEORY FOR AUGER INTENSITIES

A. Auger rate for muffin-tin orbitals

In this section we will derive calculable expressions for the effective one-electron scheme justified in the preceding section.

We begin by considering the Auger rate from the central core-hole cell "0." We adopt the muffin-tin or atomic-sphere (ASA) approximation and write the orbitals as

$$\phi_k(\mathbf{r})=\sum_L i^l B_L^k Y_L(\hat{\mathbf{r}})\phi(\varepsilon_k,r) \ . \tag{19}$$

Here L is a shorthand collective index for the angular momentum labels (l and m) and k is short for the valence-electron labels. Making the usual multipole expansion of the Coulomb interaction $v(\mathbf{r}-\mathbf{r}')=1/|\mathbf{r}\cdot\mathbf{r}'|$ we obtain the central-cell part of the matrix elements as

$$\langle kk'|v|cA\rangle_0=\sum_{LL',L_A,L''} i^{l_A-l-l'}(B_L^k B_{L'}^{k'})^* B_{L_A}^{k_A}\langle Y_L|Y_{L''}Y_{L_c}\rangle\langle Y_{L'}Y_{L''}|Y_{L_A}\rangle R_{l''}(\varepsilon l,\varepsilon',l',c,A)\delta_{ss_c}\delta_{s's_A} \tag{20}$$

where

$$R_k(a,b,c,d)=\int_0^S dr\int_0^S dr'\frac{r_<^k}{r_>^{k+1}}P_a(r)P_b(r')P_c(r)P_d(r') \tag{21}$$

is a Slater integral and P_a an r-multiplied radial wave function (S is the sphere radius). To proceed further we rewrite the Auger rate in Eq. (3) as

$$D_A(\varepsilon_A)=2\pi\int_{-\infty}^{\mu}d\varepsilon\int_{-\infty}^{\mu}d\varepsilon'\sum_{k,k'}\sum_{k_A}\delta(\varepsilon-\varepsilon_k)\delta(\varepsilon'-\varepsilon_{k'})\delta(\varepsilon_A-\varepsilon_{k_A})\delta(\varepsilon+\varepsilon'-\varepsilon_c-\varepsilon_A)$$
$$\times(|\langle kk'|v|cA\rangle|^2-\langle kk'|v|Ac\rangle^*\langle kk'|v|cA\rangle) \ .$$

When we insert the actual matrix elements, Eq. (20), in the expression above, we encounter sums like

$$\sum_k \delta(\varepsilon-\varepsilon_k)B_L^k(B_{\bar{L}}^k)^* \ .$$

For angular momenta less than 2, these sums are diagonal in m and $\bar{m}$ and independent of m. Thus, we have

$$\sum_k \delta(\varepsilon-\varepsilon_k)B_L^k(B_{\bar{L}}^k)^*=\frac{1}{2l+1}D_l(\varepsilon)\delta_{L\bar{L}} \ , \tag{22}$$

where

$$D_l(\varepsilon)=\sum_{k,m}|B_L|^2\delta(\varepsilon-\varepsilon_k) \tag{23}$$

is the projected density of states (PDOS) per spin at the impurity site. Here we assume Eq. (22) to be valid also for higher angular momenta, thereby making a small error for d and higher contributions. For simple metals, however, we will see that these contributions are small.

When we make the approximation in Eq. (22), all sums over m labels can be done analytically. We express the overlaps of spherical harmonics in terms of Wigner 3-j symbols. After averaging over the core-hole magnetic (and spin) sublevels we find, making use of orthogonality properties, that the sum of Wigner coefficients in the direct term reduces to a sequence of 3-j coefficients with m indices equal to zero. The sum over m labels can also be carried out analytically for the exchange term. After some algebra one finds that the sequence of Wigner coefficients in that term nicely combines into a Wigner 6-j symbol. The final result we write as

$$D_A(\varepsilon_A)=2\pi\int_{-\infty}^{\mu}d\varepsilon\int_{-\infty}^{\mu}d\varepsilon'\sum_{l,l',l_A}D_l(\varepsilon)D_{l'}(\varepsilon')D_{l_A}(\varepsilon_A)M_{ll'l_A}(\varepsilon,\varepsilon',\varepsilon_A)\delta(\varepsilon+\varepsilon'-\varepsilon_c-\varepsilon_A) \ . \tag{24}$$

The quantity M contains the radial matrix elements and Wigner coefficients. Its direct and exchange parts are, respectively,

$$M^{(d)}_{ll'l_A}(\varepsilon,\varepsilon',\varepsilon_A)=2\sum_k \frac{1}{2k+1}\begin{bmatrix} l & l_c & k \\ 0 & 0 & 0\end{bmatrix}^2\begin{bmatrix} l' & l_A & k \\ 0 & 0 & 0\end{bmatrix}^2 |R_k(\varepsilon l,\varepsilon' l',c,\varepsilon_A l_A)|^2 , \tag{25}$$

$$M^{(x)}_{ll'l_A}(\varepsilon,\varepsilon',\varepsilon_A)=-\sum_{k,k'}\begin{bmatrix} l & l_c & k \\ 0 & 0 & 0\end{bmatrix}\begin{bmatrix} l' & l_A & k \\ 0 & 0 & 0\end{bmatrix}\begin{bmatrix} l & l_A & k' \\ 0 & 0 & 0\end{bmatrix}\begin{bmatrix} l' & l_c & k' \\ 0 & 0 & 0\end{bmatrix}$$
$$\times(-1)^{k+k'}\begin{Bmatrix} l & k & l_c \\ l' & k' & l_A\end{Bmatrix} R_k(\varepsilon l,\varepsilon' l',c,\varepsilon_A l_A)R^*_{k'}(\varepsilon l,\varepsilon' l',\varepsilon_A l_A,c) . \tag{26}$$

This completes our derivation of the Auger intensity from the central cell.

The Auger matrix element $\langle kk'|v|cA\rangle$ has contributions also from those parts of the orbitals $\phi_{k'}$ and ϕ_{k_A} which are outside the central cell. When forming the Auger intensity of the complete matrix elements, we also obtain, in addition to the central-cell contribution given above, two- and three-center terms. Such terms have been estimated by Matthew and Komninos[30] and have been found to be very small. We have also made estimates which confirm that the interatomic terms are small for the systems considered here.

B. Treatment of the Auger-electron orbital

In previous works different prescriptions for obtaining the Auger-electron orbitals have been used. Thus Feibelman and co-workers[20] argue that one should use an orbital corresponding to a doubly charged ion in vacuum. A similar prescription has been used by Jennison and coworkers.[21] von Barth and Grossmann[19] solved the Auger orbital in the same effective potential as was used for the valence orbitals within the central atomic sphere and matched this solution to free spherical wave outside the cell. The above works were concerned with line shapes, but the question of how to approximate the Auger orbitals is important also when total rates are calculated.

Let us first consider the problem of finding reasonable approximations to the potential. For a free atom the obvious and commonly used approximation is to take the potential as that corresponding to the doubly charged ion left behind.[31] For a solid, on the other hand, the situation is rather different. Here the initial state is the fully relaxed core-hole state with essentially no net charge within the central cell, in the case of metals, and with some uncompensated charge in the case of semiconductors or insulators. Using a time-scale argument, Feibelman *et al.*[20] propose that the Auger electron also in a solid is seeing a doubly charged central cell left behind like in the case of atoms. The question of choosing the "best" one-electron potential is of course a complex and basically unsolved many-body problem, but we believe that Feibelman's description overestimates the hole effects. If we could measure the charge density in the central cell as a function of time after adding both a core and an Auger electron and annihilating two valence electrons with the appropriate amplitudes ($\langle cA|v|kk'\rangle$), we would in fact see a *continuous* change. The central-cell charge would first increase by about one unit on a time scale given by the Auger-electron velocity. The charge would then tend to its ground-state value on a time scale given by the valence-electron hopping time. However, the uncertainty principle makes it impossible to simultaneously measure the energy distribution of the Auger electrons. In order to obtain the energy-resolved Auger current we must decompose the transition state in question,

$$V_A|0\rangle=\sum_{k,l,A}\langle cA|v|kl\rangle b^\dagger c^\dagger_A c_l c_k|0^*\rangle ,$$

into exact no-hole eigenstates. In order to form a wave packet of exact eigenstates having a charged central cell, higher shakeup states are required, and thus we believe that the final ground-state potential with no core hole is a reasonable first-order approximation to use in the no-loss part of the current closer to the threshold. Away from the threshold, higher excited states contribute and give losses, both of intrinsic and extrinsic nature, and we are dealing with phenomena outside a one-electron picture.

In the case of total rates we may base our discussion on the initial state rule, Eq. (10). This expression implicitly involves the no-hole Hamiltonian [cf. Eq. (7)]. Taking the final states as Slater determinant of no-hole orbitals and neglecting the small overlaps between the final-state Auger orbital and the initial-state valence orbitals, as well as the weak energy dependence of the matrix elements, one obtains the usual one-electron expressions, Eq. (3), but with relaxed valence orbitals and unrelaxed Auger orbitals. We have performed test calculations both with relaxed and unrelaxed Auger orbitals and have found only minor differences, and for simplicity we then solved all orbitals using the initial-state potential. The effective one-electron approximation used here clearly leaves out dynamical effects arising from interactions between the Auger electron and the correlated hole state left behind. However, at high kinetic energies these vertex corrections are generally believed to be small.

Having discussed the physical basis of our effective potential we now turn to the more practical question of computing the corresponding orbitals. Let us consider a calculation based on the ground-state potential. Neglecting surface effects, the orbitals have Bloch symmetry with unit norm in every cell. It is quite a difficult task to obtain such orbitals at energies of the order 100 eV. To

TABLE I. Error measures for different approximations to Auger orbitals. N is the central-cell norm of the equivalent scattering state in the spherical approximation; Δ and ΔE are error measures for the LAPW approximation as defined in Eqs. (27) and (28).

	Spherical waves	LAPW					
	N	Δ_s	Δ_p	Δ_d	ΔE_s	ΔE_p	ΔE_d
Li KVV	1.09	0.195	0.345	0.161	0.61	−0.84	−0.42
Be KVV	1.08	0.314	0.374	0.155	1.34	−1.05	−0.81
Na $L_{2,3}VV$	1.17	0.063	0.032	0.480	0.24	−0.13	−0.25
Mg $L_{2,3}VV$	1.19	0.112	0.021	0.733	0.51	−0.18	−0.39
Mg KVV	1.03	0.041	0.811	0.688	1.04	2.08	−2.54
Al $L_{2,3}VV$	1.16	0.283	0.015	0.744	0.89	−0.23	−0.66

compare the approximation of matching solutions inside the central cell to free waves with the more appropriate Bloch-wave approach, we make a unitary transformation and form a scattering state $\psi_{\mathbf{k}}$ of the spherical waves with the long-range behavior

$$\psi_{\mathbf{k}} \sim (V_c)^{-1/2} \left[e^{i\mathbf{k}\cdot\mathbf{r}} + f_{\mathbf{k}}(\hat{\mathbf{r}}) \frac{e^{ikr}}{r} \right] .$$

The scattering states and the spherical waves give identical results for the angular-integrated Auger intensity. Because the Bloch symmetry has not been imposed, the scattering state may have a norm within the central cell which is different from 1. We may take this difference as a crude measure of the error we are making in this approximation. These values are shown in Table I. We see that the violation in norm is typically of the order 15% for Auger-electron energies of the order 50–100 eV. Those partial waves which actually couple to s- and p-valence states, i.e., the Auger-electron s, p, and d waves (cf. Table II) only contribute some 30% to the central-cell norm at these energies. This contribution decreases with

TABLE II. Vector-coupling coefficients according to Eqs. (25) and (26) for core levels of s and p symmetry for the direct (C_d) and the exchange (C_x) parts.

l_c	l	l'	l_A	k	k'	C_d	C_x
0	0	0	0	0		1	
	0	0	0	0	0		1
	0	1	1	0		$\frac{1}{3}$	
	0	1	1	0	1		$\frac{1}{9}$
	1	0	1	1		$\frac{1}{27}$	
	1	0	1	1	0		$\frac{1}{9}$
	1	1	0	1		$\frac{1}{27}$	
	1	1	0	1	1		$\frac{1}{27}$
	1	1	2	1		$\frac{2}{135}$	
	1	1	2	1	1		$\frac{2}{135}$
1	0	0	1	1		$\frac{1}{27}$	
	0	0	1	1	1		$\frac{1}{27}$
	0	1	0	1		$\frac{1}{27}$	
	0	1	0	1	0		$\frac{1}{9}$
	0	1	2	1		$\frac{2}{135}$	
	0	1	2	1	2		$\frac{2}{225}$
	1	0	0	0		$\frac{1}{3}$	
	1	0	0	0	1		$\frac{1}{9}$
	1	0	2	2		$\frac{2}{375}$	
	1	0	2	2	1		$\frac{2}{225}$
	1	1	1	0		$\frac{1}{9}$	
	1	1	1	0	0		$\frac{1}{27}$
	1	1	1	0	2		$\frac{2}{135}$
	1	1	1	2		$\frac{2}{1125}$	
	1	1	1	2	0		$\frac{2}{135}$
	1	1	1	2	2		$\frac{4}{6750}$

increasing Auger-electron energy, and as the higher-l waves are largely unaffected by the potential we expect the spherical-wave approximation to work better and better with increasing energy.

To be able to judge the quality of the spherical-wave approach, we have also approximated the Auger orbital by a single linear augmented plane wave (LAPW).[32] In this scheme a radial wave function (P) is a linear combination of a proper solution (P_ν) and its energy derivative ($P_{\dot\nu}$) at a fixed energy E_0 which we choose as the Auger-electron mean energy:

$$P = A(P_\nu + \omega P_{\dot\nu}) .$$

As an error measure in this approach we may use the squared norm (Δ) of that part which is not a proper eigensolution,

$$\Delta = |A\omega|^2 \langle P_{\dot\nu}|P_{\dot\nu}\rangle , \tag{27}$$

or the expectation value

$$\Delta E = \langle P|(H-E)|P\rangle . \tag{28}$$

These quantities are also given in Table I. For the $L_{2,3}VV$ spectra of Na, Mg, and Al the error is tolerably small for the s and p waves but not for the d wave. However, we see in Table II that the d wave couples rather weakly to the valence states, and thus the error in the d-wave part of the Auger orbital is not expected to influence the spectrum in any important way. We have found that the two different approximations give similar line shapes in these cases, whereas the total yields are somewhat more sensitive. Compared with the treatment of the valence states, our approximations for the Auger orbitals are rather crude. Nevertheless, the agreement is good enough to give us confidence in the approximations used.

In the case of the KVV spectra of Li, Be, and Mg we see that the error involved in the LAPW scheme is quite large also for the p wave, whereas the error measure used for the spherical-wave approach is actually smaller than in the $L_{2,3}VV$ spectra discussed above. Thus the latter approximation is to be preferred here. This scheme is further supported by a recent calculation by Müller and Wilkins,[33] who find that the PDOS from the simple spherical-wave method agree quite well with suitably broadened full LAPW results at energies in the range of interest here.

IV. ONE-PARTICLE THEORY OF RADIATIVE RATES

We first derive the radiative rates according to the length formula, and transform to the velocity form at the end of this section. The radiative width according to the length formula is given by

$$\Gamma_r \equiv \langle 0^*|\hat\Gamma_r|0^*\rangle = \int I(\omega)d\omega ,$$

where

$$I(\omega)\equiv I^{(r)}(\omega)=2\pi\sum_{f,q}|\langle f|a_q V_r|0^*\rangle|^2\delta(\omega_q+E_f-E_0^*)\delta(\omega-\omega_q)=\tfrac{4}{3}\alpha^3\omega^3\sum_{j=1}^{3}\sum_f|\langle f|R_j|0^*\rangle|^2\delta(\omega+E_f-E_0^*) .$$

Here R_j is a Cartesian component of $\sum_n \mathbf{r}_n$, and α is the fine-structure constant, $\alpha\approx\frac{1}{137}$. Specializing to one-particle theory and to cubic symmetry the length formula simplifies to

$$I^{(r)}(\omega)=4\alpha^3\omega^3\sum_k^{\text{occ}}|\langle k|z|c\rangle|^2\delta(\varepsilon_c+\omega-\varepsilon_k) .$$

Taking ϕ_k to be a muffin-tin wave function this can be simplified further by a similar technique, as was used above for the Auger rates. In the present case the reduction is much simpler and details are available in the literature, so we just give the final result

$$I^{(r)}(\omega)=\tfrac{4}{3}\alpha^3\omega^3\sum_l D_l(\varepsilon_c+\omega)\times\Theta(\mu-\varepsilon_c-\omega)\begin{bmatrix} l & l_c & 1\\ 0 & 0 & 0\end{bmatrix}^2\times Q_1(\varepsilon l,c) . \tag{29}$$

Here D_l is as before the PDOS for one spin at the core-hole site, and

$$Q_1(a,b)=\int_0^S P_a(r)rP_b(r)dr \tag{30}$$

is the radial matrix element.

Provided we use the actual one-electron eigenvalues ε_k and ε_c^0, the length and the velocity formulas give the same result for local potentials. If we instead use the experimental core-electron energy ε_c or a theoretical value computed by other means, the velocity formula gives a result which differs from Eq. (29) by the factor

$$I^{(v)}(\omega)/I^{(r)}(\omega)=\frac{(\omega+\varepsilon_c-\varepsilon_c^0)^2}{\omega^2} . \tag{31}$$

The difference between the length and velocity results is no consequence of our basic description, expressed in Eqs. (4)–(6), but occurs because we compute spectra from variational estimates to the eigenstates in the subspaces $n_c=0$ and $n_c=1$. The velocity form is less sensitive to the core energy ε_c and is generally believed to be more accurate in nonconserving approximations.

V. THE REPEATED-CLUSTER METHOD FOR IMPURITIES

In this section we will give some further details concerning our one-electron calculations. Our description here also applies in appropriate parts to the calculation of ground-state orbitals used in the following paper. As we saw in Sec. II we require wave functions corresponding to a core-hole impurity in the central cell. In a metal the core hole is screened within the central cell, and thus the impurity potential is very localized. A conceptually simple way of dealing with this problem, used earlier by von Barth and Grossmann,[19] consists of constructing a cluster of atoms, choosing one of them to contain a core hole, and repeating it so as to form an infinite solid. In this way we can perform an ordinary self-consistent band-structure calculation with this cluster as unit cell. For the band-structure problem we have used the well-known method of linear combination of muffin-tin orbitals (LMTO) which gives comparable results to any other method and is quite efficient in terms of computing time.[32] We have used the atomic-sphere approximation (ASA), and corrections to this have not been included. In the usual LMTO method the wave functions are expressed in the radial solutions and their energy derivatives at a fixed energy. In order to improve the accuracy for states far out in the Brillouin zone we have adopted a renormalization procedure due to von Barth and Grossmann.[19] Thus, after each eigenvalue diagonalization we reconstruct the wave function from radial solutions at the correct energy and the MTO expansion coefficients. In this way we obtain wave functions much closer to those obtained from the KKR-ASA (KKR denotes Korringa-Kohn-Rostoker) method. We expect to obtain accurate enough wave functions from this method with a few atoms in the cluster in view of the short screening length in free-electron-like systems.[34] In fact, we have used 15 ground-state atoms surrounding the impurity for all the systems considered here.

For the case of Na we have also compared the self-consistent supercell results for the impurity with the results obtained by using a self-consistent spherical-solid-model (SSM) potential,[34] properly modified for solids.[19] We have found that the results for the partial density of states and electron occupancies obtained by this method agree very well with the LMTO results. This gives us more confidence as far as the size of the cluster is concerned since the SSM is simulating the infinite dilution limit and is known to give good potentials for simple metals.

The clusters are chosen by doubling the size of the conventional unit cell in all directions and then choosing an appropriate primitive cell for the cluster. For the bcc systems we find a sc cluster, for the fcc systems we find a bcc cluster, and for the hcp we obtain a hcp cluster, all of them containing 16 atoms. We then solve self-consistently for all the atoms in the cluster until the root-mean-squared value for the difference in potential between two successive iterations is less than 0.001 Ry. We have used 56 **k** points in the supercell irreducible wedge for the sc cluster, 55 **k** points for the bcc cluster, and 40 **k** points for the hcp cluster. In our calculations we included up to d waves except for the Li and Na supercell calculations, where d waves were included only in the central cell. The exchange and correlation effects were included via the local-density approximation to the Hohenberg-Kohn-Sham ground-state potential[35] with electron-gas data from Ceperley and Alder.[36] After obtaining the eigenvalues and wave functions for these **k** points we calculate the density of states (DOS) in a simple approximation consisting of replacing the δ functions by Gaussians whose width is chosen typically of the order 0.01 Ry. With this procedure the finer details of the band structure are slightly broadened. For our purpose, however, these finer details disappear when forming the Auger current according to Eq. (24) by convoluting together the projected densities of states and the slowly varying radial matrix elements.

The supercell calculation is intended as an approximation of the infinite dilution limit, but due to the small size of the cluster the wave functions and charge densities will contain some spurious effects due to the interaction of the core holes at different sites. These effects, however, have been found to be rather small. For instance, the bandwidths increase by at most 6% compared to the perfect-

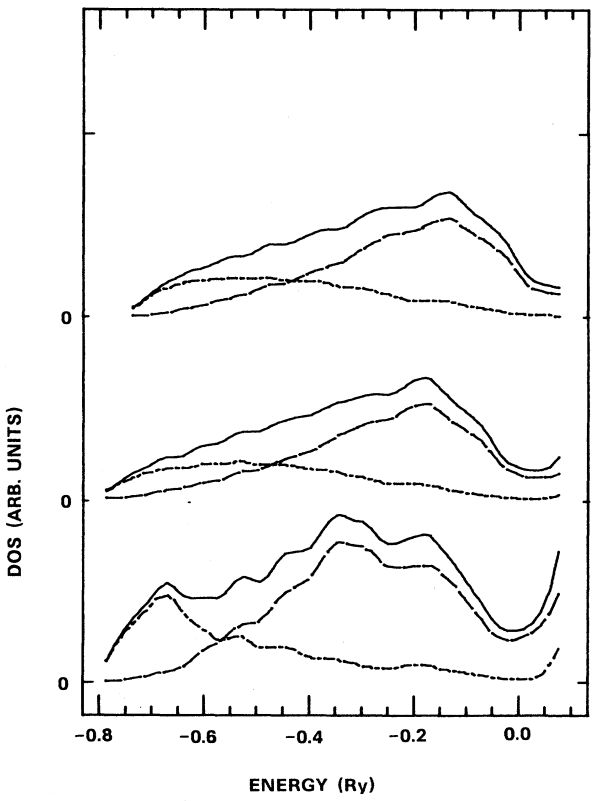

FIG. 4. Local projected densities of states below ε_F for beryllium. The top panel gives the ground state, the middle panel the average over no-hole cells when a core hole has been introduced, and the bottom panel the local DOS in the core-hole cell.

TABLE III. Number of s and p electrons in the central cell with (n_l^*) and without (n_l) a core-hole impurity according to LMTO-ASA calculations.

	Li	Be	Na	Mg 1s	Mg 2p	Al
n_s^*	0.88	0.88	1.18	1.29	1.27	1.46
n_p^*	1.23	2.03	0.78	1.56	1.52	2.14
n_s	0.52	0.63	0.64	0.88	0.88	1.11
n_p	0.48	1.25	0.36	0.94	0.94	1.48

crystal values. From the above discussion we conclude that the repeated-cluster method is providing us with sufficiently accurate wave functions for our purpose of calculating the lifetime widths.

When a core hole is introduced, the local DOS of s character changes drastically and a virtual bound state is formed at the bottom of the band. For the third-row metals the changes in shape of the local p DOS is quite small, but the case of Be (Fig. 4), and to a lesser extent Li, the changes are more pronounced. Our results for Li and Na are essentially identical to those by von Barth and Grossman[19] and need not be reproduced. The number of s and p electrons in the central cell with and without a core hole are given in Table III.

VI. RESULTS

We present our results in Table IV together with earlier theoretical and experimental results from various sources. For completeness we also give, in addition to our widths evaluated with relaxed impurity orbitals (Γ_*), the corresponding quantities (Γ_0) obtained from ground-state orbitals. For the $L_{2,3}VV$ spectra we give values obtained using both approximations for the final-state orbitals discussed in Sec. III B. The agreement between the two methods is very good for Mg and Al, whereas for Na they differ by about 20%. In the latter case we feel the LAPW method probably gives the better value due to the fairly low Auger-electron energy.

TABLE IV. Auger FWHM widths—experimental and theoretical. The labels * and 0 refer to values with and without core-hole relaxation and screening effects, respectively. Energies in meV.

Data	Element	Core level	Γ_0	$\frac{\Gamma_{ss}^0}{\Gamma_0}$	$\frac{\Gamma_{sp}^0}{\Gamma_0}$	$\frac{\Gamma_{pp}^0}{\Gamma_0}$	Γ_*	$\frac{\Gamma_{ss}^*}{\Gamma_*}$	$\frac{\Gamma_{sp}^*}{\Gamma_*}$	$\frac{\Gamma_{pp}^*}{\Gamma_*}$
SW	Li	K	4.0	0.60	0.26	0.12	17	0.32	0.32	0.35
Expt.							30±30[a]			
Expt.							16[b]			
Berg.			8[c]							
GH			46[d]							
Bose			2820[e]							
SW	Be	K	13	0.28	0.34	0.32	40	0.16	0.30	0.51
SW	Na	$L_{2,3}$	1.5	0.04	0.58	0.29	4.5	0.03	0.62	0.30
LAPW			2.2	0.13	0.57	0.21	5.7	0.15	0.62	0.18
Expt.							20±20[a]			
Expt.							10[h]			
GH			0.9[d]							
Bose			2940[e]							
KM			2.9[f]							
GF			5.2[g]							
SW	Mg	K	0.04	0.41	0.36	0.24	0.13	0.43	0.35	0.23
SW	Mg	$L_{2,3}$	5.7	0.003	0.42	0.48	12	0.004	0.43	0.49
LAPW			7.0	0.01	0.41	0.44	13	0.02	0.47	0.42
Expt.							30±20[a]			
KM			11.8[f]							
SW	Al	$L_{2,3}$	11	0.03	0.37	0.50	22	0.02	0.38	0.52
LAPW			11	0.004	0.26	0.57	22	0.002	0.34	0.54
Expt.							40±20[a]			
KM			20[f]							

[a]Citrin *et al.*, Ref. 40.
[b]Deduced as described in Ref. 5 from data by Callcott *et al.*, Ref. 42.
[c]Bergersen *et al.*, Ref. 41.
[d]Glick and Hagen, Ref. 12.
[e]Bose, Ref. 13.
[f]Kobayasi and Morita, Ref. 11.
[g]Guinea and Flores, Ref. 14.
[h]Callcott *et al.*, Ref. 39.

TABLE V. Subchannel yields compared to local occupancies for s and p electrons. The table gives the ratios $\Gamma_{ll'}/n_l n_{l'}$ in meV with (*) and without (0) a core hole. The yields correspond to the spherical-wave approximation to the Auger orbitals.

Data	Li K	Be K	Na $L_{2,3}$	Mg K	Mg $L_{2,3}$	Al $L_{2,3}$
ss^0	8.95	9.11	0.137	0.021	0.024	0.235
ss^*	7.19	8.29	0.081	0.003	0.027	0.201
sp^0	4.15	5.51	3.70	0.017	2.86	2.45
sp^*	5.05	6.69	3.03	0.023	2.70	2.64
pp^0	2.13	2.67	3.24	0.011	3.06	2.45
pp^*	4.05	5.02	2.20	0.012	2.50	2.48

As is seen in Table IV, it is of critical importance to use orbitals properly relaxed in the core-hole potential. Thus, in Li these core-hole relaxation effects increase the width by ~ 4 times. These effects have never been included before in a proper way for core-valence processes in metals. The partial contributions Γ_{ss}, Γ_{sp}, and Γ_{pp} from different "initial" valence levels are also shown. As we will see in the following paper, the relaxed values of these quantities are of importance in calculations of line shapes. Their importance comes from the fact that also the different subchannel contributions (ss,sp,pp) obey an initial-state rule as far as total yields are concerned, and thus, their relative intensities in the spectrum are governed by the ratios $\Gamma^*_{ll'}/\Gamma^*$. We see that the core-relaxation effects on these relative weights are quite important for Li and Be, whereas they are very small for the third-row metals. For Mg we notice the difference in core-hole screening effects for the K and $L_{2,3}$ yields, which indicates that the Auger process probes the electronic structure more locally when deeper core shells are involved.

In Table V we compare the subchannel yields $\Gamma_{ll'}$ with the local occupancies n_l of s and p electrons in the central cell. As anticipated, $\Gamma_{ll'}$ scales roughly with the product $n_l n_{l'}$ when a core hole is introduced. The second-row metals are exceptions, and the reason is that no core levels of p symmetry stabilize the orbitals.

When comparing with experiment we note the large experimental uncertainties which are much larger than the theoretical uncertainties we have reason to expect here. Most experimental values were obtained by analyzing XPS or SXA spectra where, as discussed previously, the lifetime part just gives a small broadening. These lifetime broadenings are very small compared to both phonon and instrumental broadenings, and are thus difficult to obtain. In the x-ray-emission spectra of Li, however, the hole lifetime determines the strong effects of incomplete lattice relaxation. When the core-hole lifetime width is of the same order as the phonon frequencies, the phonon-broadening function for Li has been shown to become very large and to acquire a two-peaked structure in a way that depends sensitively on the lifetime.[5,37] By analyzing the emission and absorption edges,[42] one of us (C.-O.A.) obtained a core-hole width of 16 meV.[5] This analysis included the full details of the phonon spectrum, but the couplings to the core hole were partily semiempirical since no reliable calculations were available at that time. These couplings have recently been confirmed in detail by Almbladh and Morales,[38] who included previously neglected but important effects of nonlinear screening. The value we obtain here, 17 meV, agrees better with the analysis in Ref. 5 than our approximation really deserves, but nevertheless it seems to be quite clear that the explanation of the Li edge proposed in Ref. 5 is the correct one.

These dynamical phonon effects discussed above seem also to be present in Na, although they are much weaker. By analyzing these effects also in Na, Callcott *et al.*[39] obtained a value of 10 meV (Table IV). Owing to the small size of the phonon effects in Na in comparison with other broadenings this value is, however, far less certain.

We also include previous theoretical work in Table IV. We note that the values are heavily scattered. We also note that all of them are to be compared to our values obtained without core-hole relaxation effects. As far as the values by Glick and Hagen and by Bose are concerned, a comparison is not really meaningful, as these authors actually do not calculate the core-hole lifetime. We observe that Bose, by a slight variation of the GH procedure, obtained a lifetime width of the $2p$ level in Na about as large as the entire valence-electron bandwidth, which again illustrates the basic incorrectness of their approach.

We finally turn to the radiative sublevel widths calculated from the velocity formula (Table VI). We notice the large screening effects for Li and Be, which again shows that the p states are rather easy to deform. The $L_{2,3}$

TABLE VI. Radiative level widths in μeV obtained with relaxed (Γ_r^*) and ground-state (Γ_r^0) orbitals.

	Li $1s$	Be $1s$	Na $2p$	Mg $2p$	Mg $1s \rightarrow V$	Al $2p$
Γ_r^0	13	170	2.8	11	1300	31
Γ_r^*	55	410	6.6	18	2300	45

yields, on the other hand, scale roughly with the number of s electrons in the central cell. The fluorescence yields Γ_r/Γ are very small, generally 0.1% or less, for the shallow core levels considered here.

VII. CONCLUDING REMARKS

The principal aim of the present paper has been to study to what accuracy Auger transitions rates in solids can be predicted, and to show that a clear picture has emerged in the theoretical description of lifetime processes in solids. For the case of Li this work in combination with Refs. 5 and 38 gives, for the first time, an *a priori* description of the Li x-ray-emission edge with no adjustable parameters which is in excellent agreement with experiment. In order to obtain reliable values we have examined crucial approximations, both of theoretical and numerical nature, needed in order to obtain calculable expressions on an effective one-electron level. Much of our discussion here applies also to calculations of Auger line shapes. We have stressed the importance of using a proper treatment of the Auger orbitals which, owing to the selection rules imposed by the Coulomb matrix elements, influence the subchannel yield ($\Gamma_{ll'}$) and thereby also the line shapes in a rather direct way. We feel the main uncertainties in our calculations lie here. We judge the approximation using a repeated cluster to obtain the impurity wave functions to be less important, at least as far as total yields are concerned. In calculations of satellite spectra from multiply ionized cores, such a treatment, however, may give, e.g., a slightly incorrect bandwidth and some structure arising from the remaining but small impurity-impurity interaction.

ACKNOWLEDGMENTS

We wish to thank Ulf von Barth for stimulating discussions. One of us (A.L.M.) acknowledges financial support from the University of Antioquia and from the International Science Programs. The present work was also supported by the Swedish Natural Science Research Council.

*Permanent address: Departamento de Física, Universidad de Antioquia, Apartado Areo 1226 Medellin, Columbia.

[1]C.-O. Almbladh and A. L. Morales, following paper, Phys. Rev. B **39**, 3503 (1989).

[2]C.-O. Almbladh and A. L. Morales, J. Phys. (Paris) Colloq. **48**, C9-879 (1987), Suppl. No. 12; in *Recent Progress in Many-Body Theories,* edited by A. J. Kallio, E. Pajanne, and R. F. Bishop (Plenum, New York, 1988), Vol. 1, p. 317.

[3]T. McMullen and B. Bergersen, Can. J. Phys. **50**, 1002 (1972).

[4]C.-O. Almbladh, Nuovo Cimento B **23**, 75 (1974).

[5]C.-O. Almbladh, Phys. Rev. B **16**, 4343 (1977); C.-O. Almbladh and P. Minnhagen, *ibid.* **17**, 929 (1978).

[6]O. B. Sokolov, V. I. Grebennikov, and E. A. Turov, Phys. Status Solidi B **83**, 281 (1977).

[7]W. Domcke and L. S. Cederbaum, Phys. Rev. A **16**, 1465 (1977).

[8]O. Gunnarsson and K. Schönhammer, Phys. Rev. B **22**, 3710 (1980).

[9]C.-O. Almbladh and L. Hedin, in *Handbook on Synchrotron Radiation,* edited by E. E. Koch (North-Holland, Amsterdam, 1983), Vol. 1b, p. 607.

[10]J. T. Yue and S. Doniach, Phys. Rev. B **8**, 4578 (1973); J. C. Fuggle, R. Lässer, O. Gunnarsson, K. Schönhammer, Phys. Rev. Lett. **44**, 1090 (1980).

[11]T. Kobayasi and A. Morita, J. Phys. Soc. Jpn. **28**, 457 (1970).

[12]A. R. Glick and A. L. Hagen, Phys. Rev. B **15**, 1950 (1977).

[13]S. M. Bose, Phys. Rev. B **19**, 3317 (1979).

[14]F. Guinea and F. Flores, J. Phys. C **14**, 2965 (1981).

[15]T. Åberg, Phys. Scr. **21**, 495 (1980); T. Åberg and G. Howat, in *Handbuch der Physik,* edited by W. Mehlhorn (Springer, Berlin, 1982), Vol. 31.

[16]U. Fano, Phys. Rev. **124**, 1866 (1961); F. H. Mies, *ibid.* **175**, 164 (1968); L. C. Davies and L. A. Feldkamp, Phys. Rev. B **15**, 2961 (1977).

[17]G. Wendin, Daresbury Laboratory Report No. DL/SCI/R11, 1978 (unpublished); M. Ohno and G. Wendin, J. Phys. B **12**, 1305 (1979).

[18]T. A. Green and D. R. Jennison, Phys. Rev. B **36**, 6112 (1987); **37**, 4246 (1988).

[19]U. von Barth and G. Grossmann, Phys. Scr. **28**, 107 (1983).

[20]P. J. Feibelman, E. J. McGuire, and K. C. Pandey, Phys. Rev. Lett. **36**, 1154 (1976); Phys. Rev. B **15**, 2202 (1977); P. J. Feibelman and E. J. McGuire *ibid.* **17**, 690 (1978).

[21]D. R. Jennison, Phys. Rev. B **18**, 6865 (1978); D. R. Jennison, H. H. Madden, and D. M. Zehner, *ibid.* **21**, 430 (1980); M. Davies, D. R. Jennison, and P. Weightman, *ibid.* **29**, 5313 (1984).

[22]For an analysis of a simple case, see C.-O. Almbladh, in *Proceedings of X84—International Conference on X-ray and Inner-Shell Processes in Atoms, Molecules and Solids, Leipzig, 1984,* edited by A. Meisel and J. Finster (Karl-Marx-Universität, Leipzig, 1984), p. 435.

[23]W. Heitler, *The Quantum Theory of Radiation,* 3rd ed. (Clarendon, Oxford, 1954).

[24]H. Feshbach, Ann. Phys. (N.Y.) **43**, 410 (1967).

[25]L. V. Keldysh, Zh. Eksp. Teor. Fiz. **47**, 1515 (1964) [Sov. Phys.—JETP **20**, 1018 (1965)].

[26]C.-O. Almbladh, Phys. Scr. **32**, 341 (1985); Phys. Rev. B **34**, 3798 (1986).

[27]See, e.g., D. C. Langreth, in *Collective Properties of Physical Systems,* edited by B. I. Lundqvist and S. Lundqvist (Academic, New York, 1974).

[28]C. J. Powell, Phys. Rev. Lett. **30**, 1179 (1973); M. Cini, Solid State Commun. **20**, 605 (1976); G. A. Sawatzky, Phys. Rev. Lett. **39**, 504 (1977).

[29]L. Hedin, Phys. Rev. **139**, A796 (1965).

[30]J. A. D. Matthew and Y. Komninos, Surf. Sci. **53**, 716 (1975).

[31]E. J. McGuire, in *Atomic Inner-Shell Processes,* edited by B. Crasemann (Academic, New York, 1975), Vol. 1, p. 293.

[32]O. K. Andersen, Phys. Rev. B **12**, 3060 (1975).

[33]J. E. Müller and J. W. Wilkins, Phys. Rev. B **29**, 4331 (1984).

[34]C.-O. Almbladh and U. von Barth, Phys. Rev. B **13**, 3307 (1976).

[35]P. Hohenberg and W. Kohn, Phys. Rev. **136**, B864 (1964); W.

Kohn and L. J. Sham, *ibid.* **140**, A1133 (1965).
[36]D. M. Ceperley and B. J. Alder, Phys. Rev. Lett. **45**, 566 (1980).
[37]G. D. Mahan, Phys. Rev. B **15**, 4587 (1977).
[38]C.-O. Almbladh and A. L. Morales, J. Phys. F **15**, 991 (1985).
[39]T. A. Callcott, E. T. Arakawa, and D. L. Ederer, Phys. Rev. B **18**, 6622 (1978).
[40]P. H. Citrin, G. K. Wertheim, and Y. Baer, Phys. Rev. B **16**, 4256 (1977).
[41]B. Bergersen, P. Jena, and T. McMullen, J. Phys. F **4**, L219 (1974).
[42]T. A. Callcott, E. T. Arakawa, and D. L. Ederer, Phys. Rev. B **16**, 5185 (1977).

View publication stats